Central Asian Journal of Medical Sciences
CAJMS

Original Article

Cent Asian J Med Sci. 2018 Dec; 4(4):281-292. https://doi.org/10.24079/CAJMS.2018.12.006

# Antineoplastic Properties of Phyto-synthesized Silver Nanoparticles from Hibiscus Sabdariffa Linn. Bark Extract

**Majidul Islam, Rumana Yesmin, Hanif Ali, Ayshasiddeka, Polash Chandra Karmakar, Rowshanul Habib, A. K. M. Asaduzzaman, Tanzima Yeasmin**

Department of Biochemistry and Molecular Biology, Faculty of Science, University of Rajshahi, Rajshahi 6205, Bangladesh

**Submitted:** November 20, 2018
**Revised:** December 5, 2018
**Accepted:** December 11, 2018

**Corresponding Author**
Tanzima Yeasmin, PhD, Professor
Department of Biochemistry and Molecular Biology, Faculty of Science, University of Rajshahi, Rajshahi 6205, Bangladesh
**Tel:** +88-01556312361
**Fax:** +88-0721-750064
**E-mail:** yeasmin_bio@ru.ac.bd



**Objectives:** In recent years, green synthesis of silver nanoparticles (AgNPs) has gained much interest from researchers as biomedical treatments. The purpose of this study was to determine if AgNPs synthesized from Hibiscus Sabdariffa L. bark extract are an effective stabilizing agent and inhibit Ehrlich ascites carcinoma (EAC) cell growth. **Methods:** AgNPs were prepared by the reaction of 0.6mM silver nitrate and 5% bark extract. Synthesis of AgNPs were confirmed by UV-visible spectroscopy as well as characterized by scanning electron microscopy, x-ray diffraction, and fourier transform infrared spectroscopy. AgNPs was applied on 1,1-diphenyl-2-picrylhydrazyl (DPPH) and 2,2'-azino-bis (3-ethylbenzothiazoline-6-sulphonic acid) (ABTS) experiments to determine its antioxidant activity as well as its cytotoxic effect against EAC cells. In vivo, the antineoplastic effect of AgNPs was tested against EAC cells. **Results:** The synthesized AgNPs have a surface plasmon resonance band centered at 475 nm. Fourier transform infrared spectroscopy (FTIR) spectra showed major peaks of phytochemicals and proteins involved in AgNPs biosynthesis by identifying different functional groups involved in effective capping of AgNPs. The scanning electron microscope (SEM) analysis of AgNPs showed spherical nanoparticles with mean size 90.82 nm. The DPPH and ABTS assays revealed the antioxidant activity of AgNPs with $IC_{50}$ 31.74±2.06 and 15.45±2.72 µg/ml that was comparable to catechin. The synthesized AgNPs exhibited effective cytotoxic activity against EAC cells and the inhibitory concentration ($IC_{50}$) was recorded at 32.00 µg/ml. AgNPs showed effective cell growth inhibition, increased life span, reduced tumor weight, restored all hematological characteristics to normal level and also induced apoptosis of EAC cells. **Conclusion:** This study proves that the phyto-synthesized AgNPs show effective anticancer properties against EAC cells.

**Keywords:** Hibiscus Sabdariffa, Silver Nanoparticle, Green Synthesis, UV-Visible, Bark Extract.

## Introduction

Plant mediated synthesis of silver nanoparticles (AgNPs) has been emerged as one of the important branches of current bionanotechnology because biosynthesis of AgNPs using plant materials is easy, efficient and eco-friendly in comparison to chemical-mediated or microbe-mediated synthesis of AgNPs. Plants contains biomolecules like proteins, phenols, saponins and flavonoids play that not only a role in reducing the ions into particles but also play an important role in the capping of nanoparticles. Plant extract synthesized silver nanoparticles (AgNPs) have been shown to possess better antimicrobial activities against a wide range of microorganisms including multidrug resistant bacteria and yeast pathogens[1]. AgNPs have been shown to be effective against a broad range of human cancers such as lung, cervical, breast, and colon cancer because the water-soluble organic moieties in the nanoparticles induce a synergistic antiproliferative effect in various cancer cell lines, and thus have proven useful in various types of cancer treatments[2-6]. AgNPs have been found to induce the apoptotic pathway in vitro through free oxygen radical generation, which has antitumor, antiproliferative and antiangiogenic effects in vitro[7]. Compounds having antiangiogenic properties are known for their potential to hinder the action of abnormally expressed signaling proteins, for example, Ras and Akt, and thus subsequently have a reliable antitumor effect[8].

*Hibiscus sabdariffa L.* (family Malvaceae) is commonly known as Roselle or Rosella fruit. The red calyces of roselle plant are widely used as food and beverages in a number of tropical countries. The leaves of roselle plant are used as vegetable in the northeastern Indian state of Assam, and the plant is locally known as Mesta or Tengamora in Assamese. The roselle petals are reported to be rich source of anthocyanins, L-ascorbic acid, anisaldehyde, b-carotene, b-sitosterol, citric acid, malic acid, cyanidin-3 rutinoside, delphinidin, galactose, gossypetin, hibiscetin, mucopolysaccharide, pectin, protocatechuic acid, polysaccharide, quercetin, stearic acid, and wax[9-12]. The roselle petals have antioxidant activity and has been used to treat hypertension[9,13,14]. They also a rich source of gamma-tocopherol[15]. Since roselle petal extracts contain a significant amount of organic acids, including citric acid, hydroxycitric acid, hibiscus acid, malic, and tartaric acids as major compounds, and oxalic and ascorbic acid as minor compounds, it can be used as reducing agent[16].

*Hibiscus sabdariffa* is a strongly basic dye with a large number of medicinal applications and is used for various diagnostic purposes. The iron (Fe) nanoparticles synthesized from flower extract of *Hibiscus sabdariffa* Linn showed a higher photocatalytic degradation activity[17]. *Hibiscus Sabdariffa*'s flower extract acts as an effective chelating agent in the synthesis of $CeO_2$ nanoparticles[18]. The AgNPs synthesized from leaf extract of *Hibiscus sabdariffa* are effective in catalyzing the reduction of 4-nitrophenol[19]. Gold nanoparticles synthesized from leaf and stem extract of *Hibiscus sabdariffa* show selective toxicity towards U87 glioblastoma multiforme cell line under normal and hyperglycemic condition[20].

To the best of our knowledge, there is no report on the synthesis of AgNPs from *Hibiscus sabdariffa L.* bark so far. Hence the present study is undertaken to synthesize stable silver nanoparticles from bark extract of *Hibiscus sabdariffa* and test their antioxidant and anticancer potential after their characterization using advanced tools.

## Materials and Methods

### Chemicals

Silver Nitrate ($AgNO_{3)}$, potassium bromide, 1,1-diphenyl-2-picrylhydrazyl (DPPH), potassium ferricyanide, phosphate buffer, catechin (CA), ferrous ammonium sulphate, butylated hydroxytoluene (BHT), gallic acid (GA), ascorbic acid (AA), trichloro acetic acid (TCA), sodium phosphate, ammonium molybdate, DMSO, EDTA, thiobarbituric acid (TBA) and $FeCl_3$ were purchased from Sigma-Aldrich (St. Louis, MO, USA) whereas Folin-Ciocalteus's phenol reagent (FCR) and sodium carbonate were obtained from Merck (Darmstadt, Germany). Penicillin-streptomycin and fetal calf serum were obtained from Bangladesh distributor of Invitrogen (USA). Methanol and other solvents were purchased from E-Mark (Germany) and all the chemicals used here were of analytical and HPLC grade with 99.9% purity.

### Collection of plant materials and authentication

The bark of *Hibiscus sabdariffa L.*. was collected from the campus area of Rajshahi University, Bangladesh. Authentication of the plant material was done by a taxonomist at the Department of Botany, University of Rajshahi. The voucher sample (No. 12)

of this collection was deposited for further reference. Plant materials (1 kg) were then washed with double-distilled water to remove dirty materials and shade dried for several days, with occasional sun drying. The dried materials were ground into coarse powder, passed through sieve #40 and stored at room temperature for future use.

**Synthesis of silver nanoparticles**

Five grams of fine powder bark of Hibiscus sabdariffa along with 100 ml of distilled water was mixed and decanted. The extract was filtered with Whatman no.1 filter paper, stored at 4 LC and used for further experiments. An aqueous solution (0.6 mM) of silver nitrate ($AgNO_3$) and various concentrations of bark extract from 1 to 5 ml were prepared separately. Each concentration of the bark extract was added to 10 ml of 0.6 mM $AgNO_3$ prepared solution. After 20 min, the color of the solution changed from light yellow to dark brown, indicating the formation of AgNPs. The resulting colloidal solution of silver was analyzed using UV-Visible spectrophotometer.

**Characterization of AgNPs**

The biosynthesized AgNPs were monitored by measuring the UV-Visible spectrum after 24 hours of reaction. A small aliquot was drawn from the reaction mixture and a spectrum was taken on a wavelength from 200 to 800 nm on UV-Visible spectrophotometer. AgNO3 solution was used as a control throughout the experiment. The synthesized AgNPs sample was freeze dried and diluted with potassium bromide (in the ratio of 1:100) to make a pellet. The Fourier transform infrared spectroscopy (FTIR) spectrum of sample was recorded on a FTIR instrument. The measurement was carried out in the range of 500–4000 cm−1 at a resolution of 4 cm−1. X-ray diffraction analysis was carried out by using an X-ray diffractometer. The sample was drop-coated onto silica plate by applying many layer of small amount of biosynthesized AgNPs on the plate with intermittent drying. This leads to a thick coat of AgNPs to be examined with monitoring the diffraction angle from 5° to 80° (2θ). The surface study of the AgNPs was examined by scanning electron microscope (SEM).

**Estimation of total phenolics**

Total phenolic contents of bark extract were estimated according to the Folin-ciocalteu reagent (FCR) method[21]. An aliquot of the extracts/a standard (0.1 mg/mL) was mixed with 2 mL Folin-Ciocalteu reagent (diluted with water 1:10 v/v) and 2 mL (75 g/L) of sodium carbonate. The reaction mixtures were vortexed for 15 sec and allowed to stand for 20 min at $25^0$C for color development. Absorbance was then measured at 760 nm UV-spectrophotometer (Shimadzu, USA). Total phenolic contents were expressed in terms of galic acid equivalent, GAE (standard curve equation: y = 0.096x+0.046, R2 = 0.999), mg of GA/g of dry extract.

**Estimation of total flavonoids**

The method of Dewanto et al. was used to estimate the total flavonoid content of bark extract with catechin used as a standard[22]. To 0.5 ml of 0.1 mg/mL extract solution, 1.5 ml of methanol, 100 µl of 10% aluminum chloride, 100 µl of 1 M potassium acetate solution and 2.8 ml of distilled water was added and then incubated for 1.5 hours at room temperature. Finally, the absorbance reaction mixture was measured at 420 nm along with different concentrations of catechin (standard). Total flavonoids content was expressed in terms of catechin equivalent, CAE (standard curve equation: y = 0.0135x + 0.0085, R2 = 0.9984), mg of CA/g of dry extract.

**Estimation of total flavanols**

Total flavanols in bark extract were estimated using the method of Kumaran and Karunakaran[23]. After mixing 2.0 ml of 0.1 mg/mL extract solution with 2.0 ml of 2% $AlCl_3$ ethanol and 3.0 ml (50 g/L) sodium acetate, the mixture was kept at 20°C for 2.5 hours and the absorbance was measured at 400 nm. Total flavanol content was expressed in terms of quercetin equivalent, QUE (standard curve equation: y = 0.0255x + 0.0069, R2 = 0.9995), mg of QU/g of dry extract.

**Estimation of total proanthocyanidins**

Determination of content of proanthocyanidins was based on the procedure reported by Sun et al[24]. After mixing 0.5 mL of 0.1 mg/mL bark extract solution with 3 mL of 4% vanillin-methanol solution and 1.5 ml hydrochloric acid, the mixture was allowed to stand for 15 minutes before absorbance was measured at 500 nm along with different concentrations of catechin (standard). Total proanthocyanidin content was expressed in terms of catechin (standard curve equation: y = 0.567x – 0.024, R2 = 0.9801), mg of CA/g of dry extract.

### DPPH radical scavenging activity

Free radical scavenging activity was determined by DPPH radical scavenging assay as described by Choi et al[25]. Three milliliters 0.1mM DPPH solution in methanol was mixed with 1 ml of AgNPs solution at different concentrations along with standard (catechin). The mixture was then vortexed thoroughly and kept in the dark place for 30 minutes at room temperature. The absorbance of the mixture was recorded at 517 nm and the percentage scavenging activity was calculated using the following formula: SA% = [(Absorbance of control– Absorbance of sample) /Absorbance of control] ×100

### ABTS radical scavenging activity

ABTS•+ radical scavenging activity of AgNPs was determined[26]. ABTS•+ was generated by reacting 7 mM ABTS stock solution with 2.45 mM potassium persulfate. The mixture was placed in the dark for 12–16 hours at room temperature. An absorbance at 734 nm of 0.70±0.02 was obtained by diluting the ABTS•+ solution with water. To different concentrations of 1 ml of test sample 3 ml of ABTS•+ solution was added and mixed thoroughly. After standing for 6 minute the absorbance was measured at 734 nm. The percentage of inhibition was measured similar to that of DPPH assay.

### Collection, administration of EAC cells and ethical clearance of mice model

Swiss albino male mice, aged 4 weeks and weighing between 25± 30 grams, were purchased from International Centre for Diarrhoeal Disease Research in Bangladesh (ICDDRB), Dhaka, Bangladesh. The animals were housed in propylene cages in a controlled environment (temperature 25±2$^0$C and 12 hours dark and light cycle) and received feed approved by ICDDRB and water ad libitum. The animals were acclimatized to laboratory conditions for 10 days prior to initiation of experiments. To keep the hydration rate constant, food and water supply were stopped 12 hours before the experiments. EAC cells were propagated intraperitoneally (biweekly) and the cells were collected from a donor Swiss albino mouse bearing 6-7 days old ascites tumors. The cells were adjusted to $1\times10^5$ cells/mL via dilution with normal saline (0.9%) and counted by hemocytometer. The viability of tumor cells was observed by trypan blue (0.4%) exclusion assay. Ethical approval and permission for using mice in our research was obtained from the Institutional Animal, Medical Ethics, Biosafety and Biosecurity Committee, Institute of Biological Sciences (225/320-IAMEBBC/IBSc), University of Rajshahi, Bangladesh.

### Cell viability test by MTT colorimetric assay

MTT colorimetric assay was used to estimate EAC cell proliferation. Cells ($2.5\times10^5$ in 200 µl RPMI 1640 media) along with extracts at various concentrations (3.125-100 µg/ml) were plated in the 96-well bottom culture plate. Then incubation was carried out at 37$^0$C for 24 hours in $CO_2$ incubator. After carefully removing the aliquot, 180 µl of PBS and 20 µl of MTT were added and again incubated at 37°C for 8 hours. 200 µl of acidic isopropanol was added into each well after removing the supernatant again. Finally, the cells were incubated at 37°C for 1 hour and the absorbance was measured at 570 nm by using titer plate reader[27].

### Determination of cell growth inhibition (in vivo)

Three groups of Swiss albino mice (n=6) weighing 26±3gm were used to estimate the cell growth inhibition properties of the extract[28]. For this purpose, on day 0, $1.6\times10^6$ EAC mice cells were inoculated into each group of mice. After 24 h of tumor inoculation, treatments were started and continued for 5 days. Groups 1 and 2 were given AgNPs at the doses of 1 and 2 mg/kg/per day, respectively, via intra-peritoneal injection. Group 3 was used as EAC-bearing control mice. On day 6, the mice were sacrificed, and viable tumor cells per mouse of the extract treated group were compared with those of control group.

### Survival time and tumor weight

Survival time and tumor weight were determined per protocol[29]. Swiss albino mice were divided into three groups (six in each group) and each group of mice received $1.6\times10^6$ EAC cells. Treatment was started after 24 hour of tumor inoculation and continued for 10 days. Groups 1 and 2 were received AgNPs at the doses of 1 and 2 mg/kg/per day, respectively whereas group 3 was used as control. Then average tumor weight gain and mean survival time (MST) of each mouse of each group was recorded.

### Studies on Hematological Parameters

Experimental mice were divided into four groups (n=6) and each mice were injected with EAC cells ($1.6\times10^6$cells/mouse)

intraperitoneally except the normal group (Group 1). Group 2 was used as control. Group 3 and group 4 mice were administered with AgNPs at 1 and 2 mg/kg/mouse/day, respectively for 10 days. On the 14th day, after tumor transplantation, tail vein blood was collected which was used to measure hematological profile[29].

### Cell morphologic change and nuclear damage

Morphological change of EAC cells in AgNPs-treated (2 mg/kg/mouse/day) and untreated control mice were investigated using a fluorescence microscope (Olympus iX71, Korea). The EAC cells from both groups of mice were collected and stained with Hoechst 33342 at 37 °C for 10 min in the dark. The cells were then washed with PBS. Finally, the morphological changes were studied using a fluorescence microscope[29].

### Statistical analysis

The data were analyzed by one-way ANOVA (analysis of variance) followed by multiple comparisons using Dunnett's post hoc test using SPSS version 16 software. All results were represented as mean ± standard deviation (SD). Differences at $p<0.05$ level were statistically significant.

## Results

### Synthesis of AgNPs

The aqueous stem bark extract of Hibiscus sabdariffa was mixed with 0.6 mM $Ag(NO_3)_2$ solutions, the color changed from brown to grey which is the primary method to confirm that the synthesized nanoparticles were silver. The color change is due to the reduction of silver ions with the help of bio molecules present in the sample[30]. Reduction of silver ions was monitored by using UV–Vis spectroscopy from 250 to 750 nm scan range. The peak obtained at 475 nm is a typical absorption peak for metallic nanoparticles which further confirms the reduced nanoparticles are silver (Figure 1).

### Characterization of silver nanoparticles

### FTIR analysis

FTIR spectroscopic study was carried out to identify the possible functional groups of the bark extract for the reduction of the $Ag^C$ and capping of the AgNPs. In the spectrum, the strong and broad peak at 3434 $cm^{i1}$ represents combined vibration frequency of –OH and $–NH_2$ groups[31]. The band at 1628.61 $cm^{-1}$ can be assigned to C-O stretching. The peak around 1384 cm-1 can be assigned to C-N stretching of amine and amides groups and the peak at 519.97 cm-1 is due to s-s stretching as shown in Figure 2[32]. Thus, the formation of $Ag^0$ nanoparticles from $Ag^C$ ions may be due to the reduction by the hydroxyl groups of the phytochemicals and amino acid and proteins present in the bark extract may be responsible for the stabilization of the AgNPs[33].

### XRD Analysis

X-ray diffraction analysis was carried out to confirm the nature

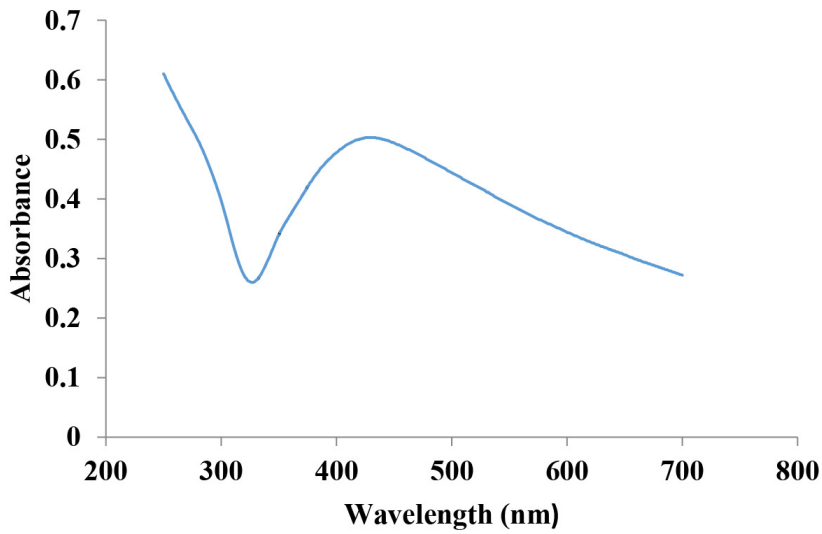


**Figure 1.** UV-Visible spectra of the synthesized AgNPs

of nanoparticles. X-ray diffraction is now a common technique for the study of crystal structures and atomic spacing. Interaction of the incident rays with the sample produced constructive interference and a diffracted ray when conditions satisfied Bragg's Law ($n\lambda=2d \sin \theta$). The freeze–dried AgNPs was drop-coated using an X-ray powder diffractometer onto silica plate by applying many layers with a small number of samples on the plate with intermittent drying. The XRD pattern shows four peaks 111, 200, 220 and 311 as shown in Figure 3.

### SEM analysis

SEM micrographs clearly displays that the green synthesized AgNPs were spherical, hexagonal in shape some particles were irregular and mostly aggregated with size 90.82 nm (Figure 4).

### Phytochemicals analysis

The stem bark extract of Hibiscus sabdariffa plant contains significant polyphenols like phenolics, flavonoids, flavonols and proanthocynidins as demonstrated in Table 1.

### Antioxidant assay of AgNPs

Considerable antioxidant activity was demonstrated by the AgNPs with respect to DPPH and ABTS inhibition. These results reveal that total antioxidant activities, DPPH as well as ABTS radical scavenging activity were increased with increasing concentration of AgNPs as shown in Table 1.

### Cytotoxic effect of AgNPs against EAC cells (in vitro)

The in vitro cytotoxicity of the AgNPs was evaluated by Ehrlich ascites carcinoma (EAC) cell lines at different concentrations. AgNPs induced EAC cell death in a dose dependent manner (Figure 5). A reduced cell growth was observed with AgNPs at a concentration as low as 3.125 µg/ml which markedly increased with increasing concentration of AgNPs compared to control. A strong inhibition (62.75%) of EAC cell growth was observed at concentration 50 µg/ml which is further increased (78.44%) at

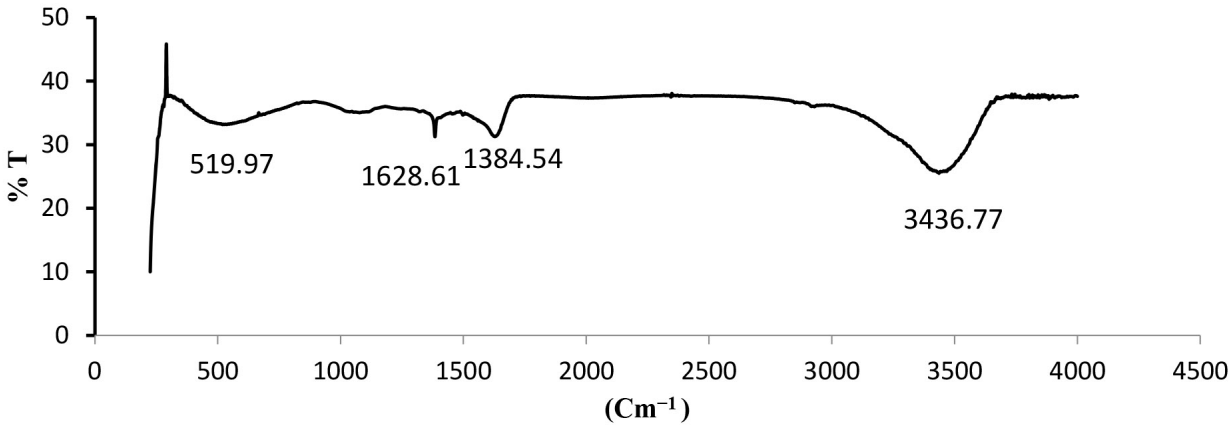


**Figure 2.** FTIR spectra of the synthesized AgNPs

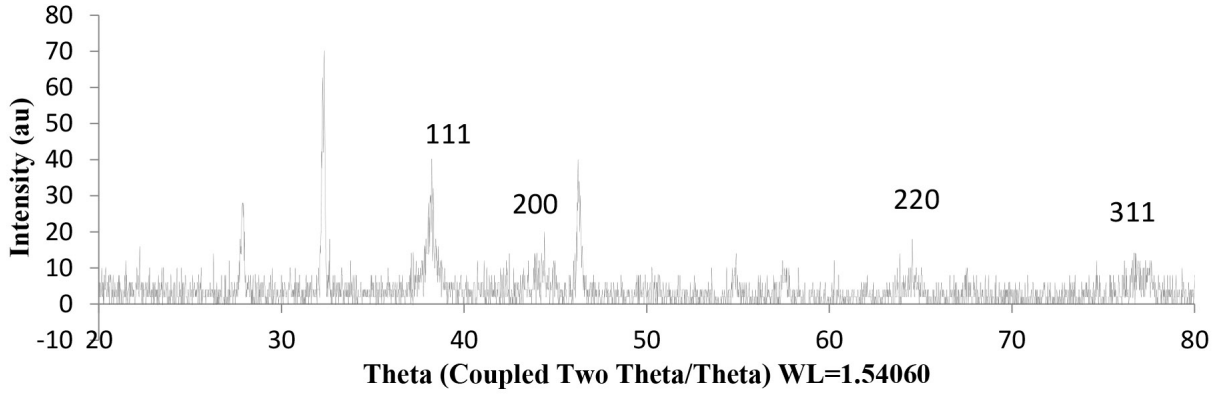


**Figure 3.** XRD patterns of the synthesized AgNPs

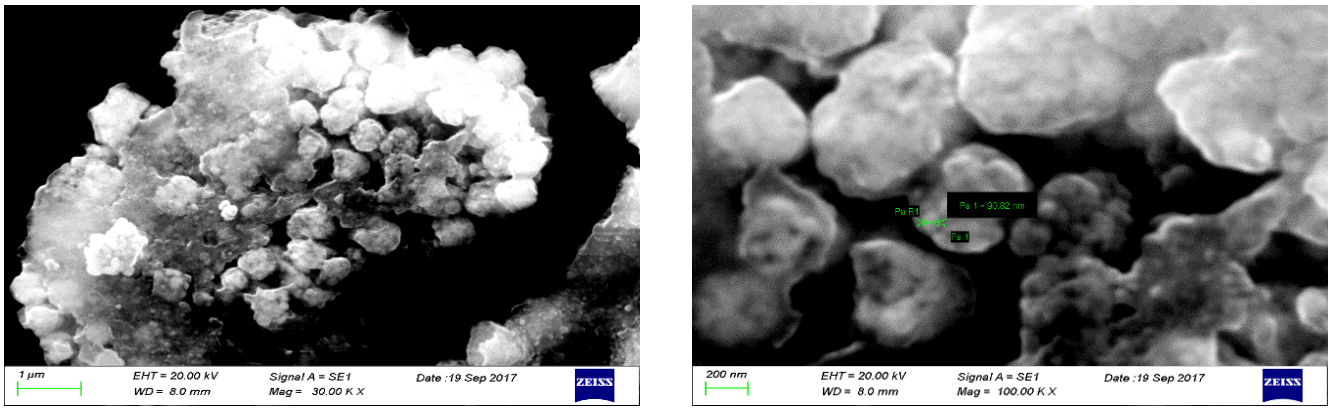


**Figure 4.** SEM observation of the synthesized AgNPs

**Table 1.** Phytochemical analysis of extract and antioxidant effect of AgNPs

| Sample | TPC (mg of gallic acid equivalent/g of extract) | TFC (mg of catechin equivalent/g of extract) | Proanthocyanidins (mg of catechin equivalent/g of extract) | Flavanols (mg of catechin equivalent/g of extract) | DPPH radical scavenging activity ($IC_{50}$ values in µg/ml) | ABTS radical scavenging activity ($IC_{50}$ values in µg/ml) |
|---|---|---|---|---|---|---|
| AgNPs | 17.35±0.98 | 65.8±2.08 | 44.44±0.96 | 5.4±0.08 | 31.74±2.06 | 15.45±2.72 |
| Catechin | - | - | - | - | 3.23±0.24 | 7.52±0.21 |

Each value is the average of three analyses ± standard deviation; TPC: Total Phenolic Content; TFC: Total Flavonoid Content

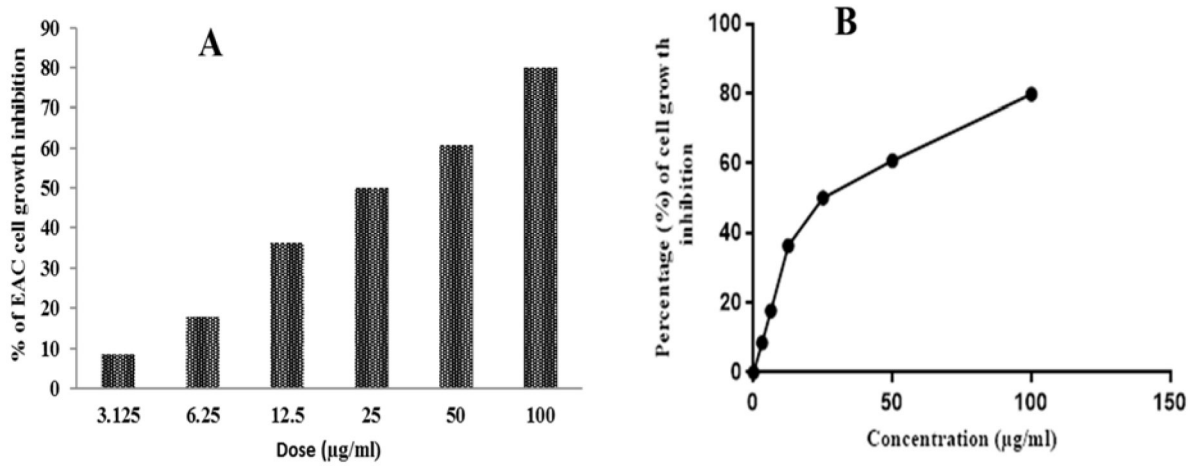


**Figure 5.** A: Growth inhibition of EAC cells by AgNPs when EAC cells were treated with various doses of AgNPs for 24 h. The inhibition ratios were measured by the MTT assay (n = 3, Mean±SD). B: $IC_{50}$ value of AgNPs was calculated from the dose–response curve.

concentration 100 µg/ml of AgNPs. The $IC_{50}$ value of the AgNPs was determined as 32.00 µg/ml against EAC cells.

### The effect of AgNPs on cell proliferation, survival time and weight gain of EAC bearing mice

The effect of AgNPs on EAC cell-induced tumorigenesis in mice and found maximum cell growth inhibition (62.91±2.04; $p<0.05$) was found after treatment with 2 mg/kg i.p. per mouse per day whereas 48.89±2.41 ( $p<0.05$) cell growth inhibition was observed at 1 mg/kg dose as shown in Table 2.

Intraperitoneal (i.p.) administration of AgNPs resulted in significant increase of mean survival time and life span of EAC-bearing mice (Table 3). At doses 1 and 2 mg/kg, EAC-bearing mice showed increased life span by 24.75±1.50%

**Table 2.** Effect of AgNPs on Ehrlich ascites carcinoma (EAC) cell growth inhibition

| Group No. | Treatment | Viable EAC cells on day 6 after inoculation (x $10^7$ cells/ml) | Percentage (%) of cell growth inhibition |
|---|---|---|---|
| 1 | EAC + Control | 3.64±0.33 | - |
| 2 | EAC + AgNPs (1 mg/kg) | 1.86±0.16* | 48.89±2.41 |
| 3 | EAC + AgNPs (2 mg/kg) | 1.34±0.06* | 62.91±2.04 |

Data are expressed as mean ± SD for six animals in each group. Data were calculated by one way ANOVA followed by Dunnett 't' test using SPSS software version 16. *p<0.05: against EAC control group.

**Table 3.** Effect of AgNPs on survival time and body weight gain of EAC cell bearing mice

| Group No. | Treatment | MST (in days) | %ILS | Body weight gain (g) after 15 days |
|---|---|---|---|---|
| 1 | EAC + Control | 20.25±1.70 | | 16.00±1.41 |
| 2 | EAC + AgNPs (1 mg/kg) | 24.75±1.50* | 22.43±4.25* | 8.00±0.81* |
| 3 | EAC + AgNPs (2 mg/kg) | 30.00±1.82* | 42.47±5.67* | 6.25±1.70* |

Data are expressed as mean ± SD for six animals in each group. Data were calculated by one way ANOVA followed by Dunnett 't' test using SPSS software version 16. * p<0.05: against EAC control group.

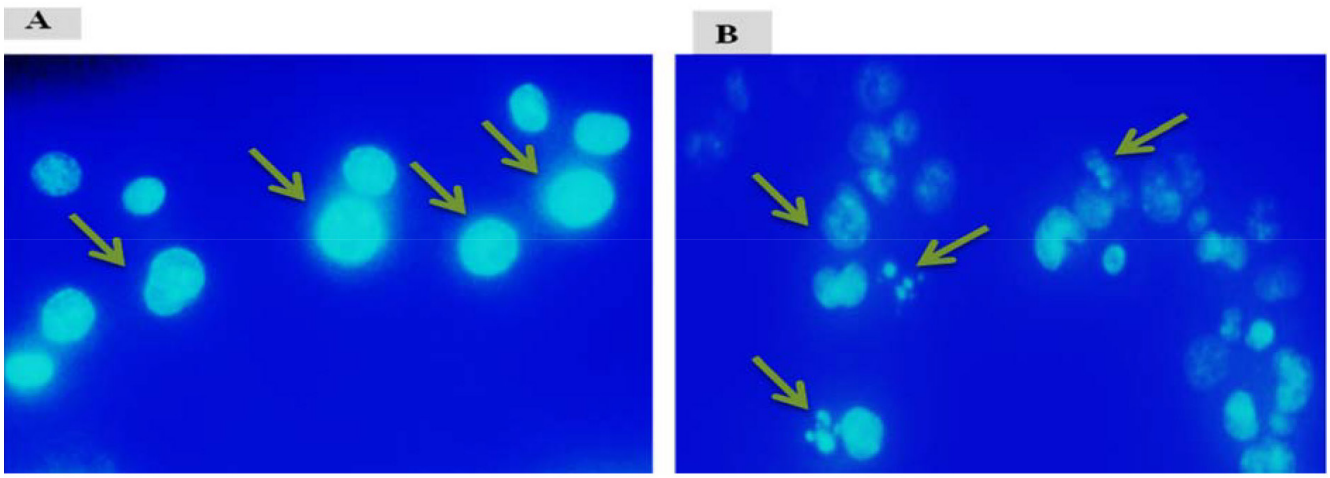


**Figure 6.** AgNPs induced apoptosis is in Ehrlich ascites carcinoma (EAC) cell. EAC cells were treated for 5 days then cells were collected from the treated and non-treated EAC-bearing mice and stained with Hoechst 33342 and observed by fluorescence microscopy. Left panel (A) indicates control and right panel (B) indicates AgNPs (2 mg/kg/day) and note that apoptotic characteristics e.g. nuclear condensation and fragmentation are seen

**Table 4.** Effect of AgNPs on blood parameters of tumor bearing Swiss albino mice

| Name of Exp. | RBC Cells (x$10^9$) /ml | WBC Cells (x$10^6$) /ml | % of Hb gm/dl |
|---|---|---|---|
| Normal mice | 14.48 ± 0.52 | 9.50±0.73 | 12.70±0.62 |
| EAC + Control | 6.67 ± 0.23 | 2.00±0.18 | 2.58±0.22 |
| EAC + AgNPs (1 mg/kg) | 8.75 ± 0.53* | 42.00±5.71* | 22.75±3.50* |
| EAC + AgNPs (2 mg/kg) | 14.48 ± 0.52* | 9.50±0.73* | 12.70±0.62* |

Data are expressed as mean ± SD for six animals in each group. Data were calculated by one way ANOVA followed by Dunnett 't' test using SPSS software version 16.* p<0.05: against EAC control group.

and 30.00±1.82%, respectively, compared with the control ($p<0.05$). AgNPs also reduced the tumor weight, compared with control group ($p<0.05$) (Table 3).

EAC cells were collected from the treated and non-treated mice, and morphological changes were studied by staining with Hoechst 33342. It was found that EAC cells nuclei of control group were round, regular, and homogeneously stained with Hoechst 33342 (Figure 6A). AgNPs treated EAC cells showed membrane and nuclear fragmentation a hall mark of apoptosis (Figure 6B). These results indicate that AgNPs could induce apoptosis of EAC cells.

On day 12, the hematological parameters of only the mice bearing the EAC cell were changed significantly when compared to normal mice. Before treatment, the WBC count of the EAC cell bearing mice were found to be increased with a reduction in hemoglobin and RBC count (Table 4). Treatment at 1 and 2 mg/kg doses, AgNPs significantly ($p<0.05$) restored all hematological characteristics to normal level.

## Discussion

This study revealed that *Hibiscus sabdariffa* stem bark extract contained high amounts of polyphenols. It has been observed that Ag+ of AgNO3 binds with polyphenols as well as other biomolecules of plant sources to form AgNPs. Different types of free radicals, including oxygen radicals and organic hydroperoxides are reported to play a significant role in cytotoxicity and carcinogenesis[34]. Many tumor promoters induce a 'pro-oxidant state' in their target tissue resulting in carcinogenic activity. Natural (vitamins C and E) and synthetic antioxidants (ethoxyquin, butylated hydroxyanisole, butylated hydroxytoluene etc.) are shown to inhibit carcinogenic chemicals by modifying their activation, detoxification and mutagenicity, in addition to their ability to scavenge reactive carcinogen metabolites and free radicals[35]. The statistical results suggest that the synthesized AgNPs have a high antioxidant potential in comparison with the standard catechin.

The cytotoxic properties of the nanoparticles are due to the release of $Ag^+$ cations which interact with cells and intracellular macromolecules like proteins and DNA. AgNPs have been shown to cause DNA damage and increased mitochondrial membrane permeability[36,37]. Cellular uptake of nanoparticles which subsequently capture free electrons and increase the synthesis and accumulation of intercellular reactive oxygen species (ROS) react with protein and cause oxidative stress[38]. This process leads to the partial or permanent loss of structure and/or function of cellular protein. It further reduced adenosine triphosphate (ATP) production[39]. In addition to enhancing the generation of potentially damaging radicals, AgNPs have also been shown to negatively regulate the activity of DNA-dependent protein kinase, a key enzyme involved in DNA damage repair via nonhomologous end joining[39]. Cell damage by silver nanoparticles may be due to loss of cell membrane integrity, apoptosis and oxidative stress.

The in vivo cytotoxicity of AgNPs was observed in EAC bearing mice model. It is known to that antioxidants neutralize free radicals, which are a natural byproduct of normal cell processes. In humans, the most common form of free radicals is oxygen. When an oxygen molecule (O2) becomes electrically charged or radicalized, it attempts to steal electrons from other molecules, causing damage to these molecules and DNA. Over time, such damage may become irreversible and lead to cancers. The results clearly indicate that AgNPs have a capacity to inhibit the growth of tumor induced by EAC cell line in the experimental animals. Once a tumor grows to a certain size, it needs nutrients and oxygen from the blood to grow and spread. The tumor sends chemical signals that stimulate the growth of new blood vessels that carry the blood to it, as growth and metastasis of tumor depend on angiogenesis[40]. Cancer treatments with AgNPs block angiogenesis, and limited angiogenesis occurs after AgNPs treatment. The tumor starves and dies if it cannot get enough nutrients and oxygen compounds reported to have anti-angiogenic properties are known for their ability to block abnormally expressing signaling proteins. Also, AgNPs have a cytotoxic effect on EAC bearing mice by production of lipid peroxidation and free radicals in tumor tissues as proved by El Bialy et al[41,42].

In MTT assay study, exposure of EAC cells to various concentrations of AgNPs for 24 hours triggered significant cell death in a dose dependent fashion (Figure 5A) which indicated the in vitro capacity of an extract to inhibit the growth of cancer cell[29].

Intraperitoneal treatment with AgNPs at the dose of 1 and 2 mg/kg body weight significantly inhibited the tumor cells volume, tumor cells count and tumor weight. In case of the control group, a regular rapid increase in ascetic tumor volume was observed.

Anemia is a problem in cancer treatment in vivo and was

encountered in tumor bearing mice in this study. This may occur either due to iron deficiency or due to hemolytic or myelopathic conditions[43].

Apoptosis, a cell-suicidal mechanism, is characterized by the change of morphological features, such as nuclear fragmentation, blebbing, cell shrinkage and chromatin condensation. Capability of selectively inducing apoptosis in cancer cells is a highly desired feature of an anticancer drug since cancer or malignant cells are selectively removed through this process without damaging normal cells. After staining with Hoechst 33342 (a blue fluorescing dye that stains), florescence microscopy enabled us to observe cell morphological features related to apoptosis such as nuclear fragmentation, chromatin condensation etc.[29] In our present study, when EAC cells were treated with AgNPs, cell shape was changed and the nucleus was fragmented and condensed; these finding were comparable with the control EAC cells suggesting that AgNPs can play significant role in cancer prevention by inducing apoptosis. Induction of apoptosis in EAC cells by different plant extracts has been identified in several previous studies[29].

Our study has some limitations. We did not identify the major compounds and molecules that are responsible for synthesizing AgNPs. In addition, this study did not confirm the details of the molecular mechanism underlying the inhibition of EAC cells by AgNPs. Further study will be conducted to isolate compounds and molecules responsible for synthesizing AgNPs and to elucidate the molecular mechanism of EAC cell inhibition.

**Conclusion**

The present data suggest that the phyto-fabricated silver nanoparticles show potential in anticancer therapeutic applications.

## Conflict of interest

The authors declare no conflict of interest.

## Acknowledgements

The authors thank IICB, Kolkata, India, authority for providing the EAC cells and the International Centre for Diarrhoeal Disease Research, Bangladesh for supplying the Swiss albino mice.

## References

1. Rajan R, Chandran K, Harper SL, Yun SI, Kalaichelvan PT. Plant extract synthesized silver nanoparticles: an ongoing source of novel biocompatible materials. Ind Crop Prod 2015; 70: 356–73.
2. Sankar R, Karthik A, Prabu A, Karthik S, Shivashangari KS, Ravikumar V. Origanum vulgare mediated biosynthesis of silver nanoparticles for its antibacterial and anticancer activity. Colloids Surf B Biointerfaces 2013; 108: 80–4.
3. Baharara J, Ramezani T, Divsalar A, Mousavi M, Seyedarabi A. Induction of apoptosis by green synthesized gold nanoparticles through activation of caspase-3 and 9 in human cervical cancer cells. Avicenna J Med Biotech 2016; 8: 75–83.
4. Mata R, Nakkala JR, Sadras SR. Polyphenol stabilized colloidal gold nanoparticles from Abutilon indicum leaf extract induce apoptosis in HT-29 colon cancer cells. Colloids Surf B Biointerfaces 2016; 143: 499–510.
5. Krishnaraj C, Muthukumaran P, Ramachandran R, Balakumaran MD, Kalaichelvan PT. Acalypha indica Linn: biogenic synthesis of silver and gold nanoparticles and their cytotoxic effects against MDA-MB-231, human breast cancer cells. Biotechnol Rep 2014; 4: 42–9.
6. Kuppusamy P, Ichwan SJA, Al-Zikri PNH, Suriyah WH, Soundharrajan I, Govindan N, et al. In vitro anticancer activity of Au, Ag nanoparticles synthesized using Commelina nudiflora L. aqueous extract against HCT-116 colon cancer cells. Biol Trace Elem Res 2016; 173: 297-305.
7. Gurunathan S, Lee KJ, Kalimuthu K, Sheikpranbabu S, Vaidyanathan R, Eom SH. Antiangiogenic properties of silver nanoparticles. Biomaterials 2009; 30: 6341-50.
8. Martins D, Frungillo L, Anazzetti MC, Melo PS, Durán N. Antitumoral activity of L-ascorbic acid-poly-D, L-(lactide-co-glycolide) nanoparticles containing violacein. Int J Nanomedicine 2010; 5: 77-85.
9. Du CT, Francis FJ. Anthocyanins of Roselle (Hibiscus sabdariffa, L.). J Food Sci 1973; 38: 810–2.
10. Faraji MH, Tarkhani, AHH. The effect of sour tea (Hibiscus sabdariffa) on essential hypertension. J Ethnopharmacol 1999; 65: 231– 6.
11. Tsai P, Mcintosh J, Pearce P, Camden B, Jordan BR. Anthocyanin and antioxidant capacity in Roselle (Hibiscus

Sabdariffa L.) extract. Food Res Int 2002; 35: 351–6.

12. Ali BH, Al Wabel N, Blunden G. Phytochemical, pharmacological and toxicological aspects of Hibiscus sabdariffa L.: a review. Phytother Res 2005; 19: 369–75.
13. Mohd-Esa N, Hern FS, Ismail A, Yee CL. Antioxidant activity in different parts of roselle (Hibiscus sabdariffa L.) extracts and potential exploitation of the seeds. Food Chem 2010; 122: 1055–60.
14. Mozaffari-Khosravi H, Jalali-Khanabadi B, Afkhami-Ardekani M, Fatehi F, Noori-Shadam M. The effects of sour tea (Hibiscus sabdariffa) on hypertension in patients with type II diabetes. J Hum Hypertens 2009; 23: 48–54.
15. Mohamed R, Fernandez J, Pineda M, Aguilar M. Roselle (Hibiscus sabdariffa) seed oil is a rich source of gamma-tocopherol. J Food Sci 2007; 72: 207–11.
16. Da-Costa-Rocha I, Bonnlaender B, Sievers H, Pischel I, Heinrich M. Hibiscus sabdariffa L.-A phytochemical and pharmacological review. Food Chem 2014; 165: 424–43.
17. Alshehri A, Malik MA, Khan Z, Al-Thabaiti SA, Hasan N. Biofabrication of Fe- nanoparticles in aqueous extract of Hibiscus sabdariffa with enhanced photocatalytic activities, RSC Adv 2017; 7: 25149-59.
18. Thovhogi N, Diallo A, Gurib-Fakim A, Maaza M. Nanoparticles green synthesis by Hibiscus Sabdariffa flower extract: Main physical properties. J Alloys Compd 2015; 647: 392-6.
19. Kalita NK, Ganguli JN. Hibiscus sabdariffa L. leaf extract mediated green synthesis of silver nanoparticles and its use in catalytic reduction of 4-nitrophenol. Inorg Nano-Met Chem 2017; 5: 788–93.
20. Mishra P, Ray S, Sinha S, Das B, Khan MI, Behera SK, et al. Facile bio-synthesis of gold nanoparticles by using extract of Hibiscus sabdariffa and evaluation of its cytotoxicity against U87 glioblastoma cells under hyperglycemic condition. Biochem Eng J 2016; 105: 264-72.
21. Singleton VL, Rossi JA. Colorimetry of total phenolics with phosphomolybdic- phosphotungstic acid reagents. Am J Enol Vitic 1965; 16: 144-58.
22. Dewanto V, Wu X, Adom KK, Liu RH. Thermal processing enhances the nutritional value of tomatoes by increasing total antioxidant activity. J Agric Food Chem 2000; 50: 3010-4.
23. Kumaran A, Karunakaran RJ. In vitro antioxidant activities of methanol extracts of five Phyllanthus species from India. Lebenson Wiss Technol 2007; 40: 344-52.
24. Sun JS, Tsuang YH, Chen IJ, Huang WC, Hang YS, Lu FJ. An ultra-weak chemiluminescence study on oxidative stress in rabbits following acute thermal injury. Burns 1998; 24: 225-31.
25. Choi HY, Jhun EJ, Lim BO, Chung IM, Kyung SH, Park DK. Application of flow injection-chemilumineacence to the study of radical scavenging activity in plants. Phytother Res 2000; 14: 250-3.
26. Cai Y, Luo Q, Sun M, Corke H. Antioxidant activity and phenolic compounds of 112 traditional Chinese medicinal plants associated with anticancer. Life Sci 2004; 74: 2157-84.
27. Bhuvaneswari R, John XR, Arumugam M. Facile synthesis of multifunctional silver nanoparticles using mangrove plant Excoecaria agallocha L. for its antibacterial, antioxidant and cytotoxic effects. J Parasit Dis 2017; 41: 180–7.
28. Khanam JA, Islam MF, Jesmin M, Ali MM. Antineoplastic activity of acetone semicarbazone (ASC) against Ehrlic ascites carcinoma (EAC) bearing mice. J Natn Sci Foundation Sri Lanka 2010; 38: 225–31.
29. Yeasmin T, Ali H, Yesmin R, Islam M, Hoshen A, Habib R, et al. Growth Inhibition and Apoptosis of Ehrlich Ascites Carcinoma Cells by Methanol Extract from the Calyx of Hibiscus Sabdariffa Linn. Cent Asian J Med Sci 2018; 4: 155-65.
30. Lalitha A, Subbaiya R, Ponmurugan P. Green synthesis of silver nanoparticles from leaf extract Azhadirachta indica and to study its anti-bacterial and antioxidant property. Int J Curr Microbiol App Sci 2013; 2: 228–35.
31. Mosmann T. Rapid colorimetric assay for cellular growth and survival: application to proliferation and cytotoxicity assays. J Immunol Methods 1983; 65: 55–63.
32. Noruzi M, Zare D, Khoshnevisan K, Davoodi D. Rapid green synthesis of gold nanoparticles using Rosa hybrida petal extract at room temperature. Spectrochim. Acta A Mol Biomol Spectrosc 2011; 79: 1461–5.
33. Cerutti PA. Prooxidant states and tumor promotion. Science 1985; 227: 375–81.
34. Da-Costa-Rocha I, Bonnlaender B, Sievers H, Pischel I, Heinrich M. Hibiscus sabdariffa L. - A phytochemical and pharmacological review. Food Chem 2014; 165: 1424–43.
35. Kahl R. The dual role of antioxidants in the modification of

chemical carcinogenesis. J. Environ Sci Hlth 1986; 4: 47–92.
36. Reddy NJ, Nagoor Vali D, Rani M, Rani SS. Evaluation of antioxidant, antibacterial and cytotoxic effects of green synthesized silver nanoparticles by Piper longum fruit. J Mater Sci Eng 2013; 34: 115–22.
37. Wang W, Irsch T. Annexin V/b5 integrin interactions regulate apoptosis of growth plate chondrocytes. J Biol Chem 2006; 281: 30848–56.
38. Almofti MR, Ichikawa T, Yamashita K, Terada H, Shinohara Y. Silver ion induce a cyclosporine a-insensitive permeability transition in rat liver mitochondria and release of apoptogenic cytochrome. CJ Biochem 2003; 134: 43–9.
39. Rahman MF, Wang J, Patterson TA, Saini UT, Robinson BL, Newport GD, et al. Expression of genes related to oxidative stress in the mouse brain after exposure to silver-25 nanoparticles. Toxicol Lett 2009; 187: 15–21.
40. Asharani PV, Mun GL, Hande MP, Valiyaveettil S. Cytotoxicity and genotoxicity of silver nanoparticles in human cells. ACS Nano 2009; 3: 279–90.
41. Dos Santos CA, Seckler MM, Ingle AP, Gupta I, Galdiero S, Galdiero M, et al. Silver nanoparticles: therapeutical uses, toxicity, and safety issues. J Pharm Sci 2014; 103: 1931–44.
42. Antony JJ, Sithika MA, Joseph TA, Suriyakalaa U, Sankarganesh A, Siva D, et al. In vivo antitumor activity of biosynthesized silver nanoparticles using Ficus religiosa as a nanofactory in DAL induced mice model. Colloids Surf B 2013; 108: 185–90.
43. Martins D, Frungillo L, Anazzetti CM, Melo PS, Durán N. Antitumoral activity of L-ascorbic acid-poly- D,L-(lactide-co-glycolide) nanoparticles containing violacein. Int J Nanomed 2010; 5: 77.